Binding modes of phosphonic acid derivatives adsorbed on TiO2 surfaces: Assignments of experimental IR and NMR spectra based on DFT/PBC calculations
Peer-reviewed author version

BINDING MODES OF PHOSPHONIC ACID DERIVATIVES ADSORBED ON TiO₂ SURFACES: ASSIGNMENTS OF EXPERIMENTAL IR AND NMR SPECTRA BASED ON DFT/PBC CALCULATIONS

D. Geldof,[a,b] M. Tassi,[b] R. Carleer,[b] P. Adriaensens,[b]
A. Roevens,[c] V. Meynen,[c] F. Blockhuys[a*]

[a]*Department of Chemistry, University of Antwerp,*
Groenenborgerlaan 171, B-2020 Antwerp, Belgium
[b] *Research Group of Applied and Analytical Chemistry, University of Hasselt,*
Agoralaan, B-3590 Diepenbeek, Belgium
[c]*Department of Chemistry, University of Antwerp,*
Universiteitsplein 1, B-2610 Antwerp, Belgium

Abstract

A DFT study on the adsorption of a series of phosphonic acids (PAs) on the TiO₂ anatase (101) and (001) surfaces was performed. The adsorption energies and geometries of the most stable binding modes were compared to literature data and the effect of the inclusion of dispersion forces in the energy calculations was gauged. As the (101) surface is the most exposed surface of TiO₂ anatase, the calculated chemical shifts and vibrational frequencies of PAs adsorbed on this surface were compared to experimental ^{31}P and ^{17}O NMR and IR data in order to assign the two possible binding modes (mono- and bidentate) to peaks and bands in these spectra; due to the corrugated nature of anatase (101) tridentate binding is not possible on this surface. Analysis of the calculated and experimental ^{31}P chemical shifts indicates that both monodentate and bidentate binding modes are present. For the reactive (001) surface, the results of the calculations indicate that both bi- and tridentate binding modes are possible. Due to the particular sensitivity of ^{17}O chemical shifts to hydrogen bonding and solvent effects, the model used is insufficient to assign these spectra at present. Comparison of calculated and experimental IR spectra leads to the conclusion that IR spectroscopy is not suitable for the characterization of the different binding modes of the adsorption complexes.

Keywords: density functional theory, titanium dioxide, phosphonic acid, adsorption, NMR spectra, IR spectra

1. Introduction

Modification of a metal oxide surface with organic components combines the stability of the inorganic material with the versatility of the organic functional groups on the surface. The resulting materials have been widely studied and have led to numerous advanced applications such as organic-inorganic membranes [1], implant biomaterials [2,3], and (dye-sensitized) solar cells [4–6]. The main issue with creating organic-inorganic materials is the interaction between the two components. Several anchor groups (thiols, carboxylic acids, alkoxysilanes, sulfonic acids, phosphonic acids, *etc.*) have been used to covalently bind the organic component to the inorganic phase; a more comprehensive list of the possible anchor groups and their interactions with metal oxide surfaces can be found in a recent review article of Pujari *et al.* [7]. The most common of these anchor groups are silanes, carboxylates and organophosphonic acids, but since organosilylated metal oxides are very susceptible to hydrolysis [8] and the bonding of carboxylates to a metal oxide surface is weak compared to other adsorbents, thereby jeopardizing their stability [9], attention has recently been shifted towards functionalization of TiO_2 surfaces with phosphonic acid derivatives (PAs) as anchor groups. The strength of P–O–Ti bonds [10–12] and the fact that PAs are easily prepared and that PA modification of the TiO_2 surface is possible in both water and organic solvents, have been cited as the main advantages.

The two most powerful experimental techniques to characterize the covalent grafting of PAs on TiO_2 are ^{31}P solid-state nuclear magnetic resonance (NMR) and infrared (IR) spectroscopy. However, the interpretation of the ^{31}P chemical shifts to distinguish mono-, bi- or tridentate binding modes [13,14] is not straightforward, because the binding mode is not the only parameter influencing the ^{31}P chemical shifts [15]. Even though IR spectra clearly indicate the presence of PAs on the surface due to the disappearance of P–O–H and P=O bands in favour of P–O–Ti bands, further characterization of the binding mode using IR spectroscopy is severely hampered by the overlap of the P–O stretching region and the bands in the native TiO_2 spectrum [13,14]. Recently, also ^{17}O NMR spectroscopy was applied to study the binding modes of PAs adsorbed on anatase [15]: this technique was able to distinguish P=O, P–O–H and P–O–Ti bonds, which led to the conclusion that multiple binding modes are possible, but that the tridentate binding mode is the most dominant. However, due to the requirement of [17]O-enriched PAs this technique is difficult to use on a routine basis.

Recently, a number of computational studies were published on PAs grafted onto TiO_2, performed to complement experimental measurements. These indicated that the most stable binding modes on the anatase (101) and rutile (110) surfaces are mono- and bidentate [16–18]. In addition, both bi- and tridentate binding modes were found to be stable on anatase (001) [17]. The latter is a minority facet [7% (001) compared to 90% (101)] but its surface is more reactive than anatase (101) [19]; in

addition, it has recently been shown that uniform anatase crystals with more than 80% of (001) can be prepared [20,21]. Despite this, its properties with respect to PA grafting have not been fully investigated.

Despite the large body of experimental and computational work performed on these systems, the precise nature of the binding modes of PAs on the surface and the associated assignments of important peaks in both NMR and IR spectra remain unclear. In this work, the binding modes of PAs on the anatase (101) and (001) surfaces will be investigated and linked to vibrational frequencies and ^{31}P and ^{17}O NMR chemical shifts. The results of the calculations will be correlated with experimental data.

2. Experimental

2.1. Computational details

All calculations were performed under Periodic Boundary Conditions (PBC) with the Quantum Espresso (QE) software package [22] using plane waves as basis sets. The Wu and Cohen functional (WC) – a modification of the PBE functional – allows for a high-quality descripton of solid-state materials and was, therefore, used throughout this work [23]. Treatment of the core electrons is based on the projector augmented wave (PAW) method [24] using the Troullier-Martins form [25]. The 1s electrons are treated as core electrons for C and O atoms, whereas P and Ti atoms are treated with the valence configurations $3s^23p^3$ and $3s^23p^64s^23d^2$, respectively. The influence of the k-point grid and cutoff was analyzed with reference to the total energy of bulk and surface anatase: a cutoff of 800 eV and a k-grid of $6 \times 6 \times 3$ were chosen. The geometry of the bulk structure was optimized until the residual forces were below 0.0002 Ry/au. The optimized bulk lattice parameters of anatase were a = 3.785 Å and c = 9.545 Å, which is in good agreement with experimental results (a = 3.789 Å and c = 9.522 Å) [26] and other calculations [27,28].

The anatase (001) and (101) surfaces were constructed using the cif2cell program [29] with a 15 Å vacuum width to avoid interactions between the slab and its image. Based on previous studies concerning the surface properties of TiO_2 in function of the number of layers, 3- and 4-layer slabs were constructed for the (101) and (001) surfaces, respectively [30–32]. A cutoff of 600 eV and a $3 \times 3 \times 1$ k-grid was chosen for the clean surfaces and adsorption complexes. The atoms in the lowest layer of the slab were constrained to their initial bulk positions, while all other layers were allowed to relax. The geometry of the clean surface and adsorption complexes was optimized until the residual forces were below 0.001 Ry/au. The geometrical parameters of the relaxed top layer of the (101) and (001) slabs are given in Table 1 with atom labels in Figure 1, and are in complete agreement with previous studies [33–35].

Calculations of the chemical shifts were performed using the Gauge-Independent Projector Augmented Waves (GIPAW) method [36], as implemented in the QE software package. The isotropic chemical shift δ_{iso} is defined as $\delta_{iso} = -(\sigma - \sigma_{ref})$, but in order to compare experimental and calculated chemical shifts, the isotropic shielding of the reference needs to be carefully selected. For the ^{31}P spectra, berlinite ($AlPO_4$) with $\delta_{iso}(^{31}P) = -24.5$ ppm [37] referenced to H_3PO_4 was chosen to define $\sigma_{ref,calc}(^{31}P)$. For the ^{17}O spectra, $\sigma_{ref,calc}(^{17}O)$ was obtained from a fit between experimental data and the calculated values for a set of SiO_2 polymorphs, a method applied in a computational study of the chemical shifts of phenylphosphonic acid which resulted in a very good agreement with the experimental data [38]. Vibrational frequencies of both the isolated molecules and the adsorption complexes were calculated at the gamma point using density functional perturbation theory, as implemented in the phonon package of the QE software package. Dispersion interactions were taken into account by adding an additional term to the DFT total energy based on the DFT-D2 method by Grimme [39,40].

2.2 Experimental details

Solid-state ^{31}P CP/MAS (cross-polarization magic angle spinning) NMR spectra were acquired at ambient temperature on an Agilent VNMRS DirectDrive 400 MHz spectrometer (9.4 T wide bore magnet) equipped with a T3HX 3.2 mm probe dedicated for small sample volumes and high decoupling powers. Magic angle spinning (MAS) was performed at 10 kHz using ceramic zirconia rotors of 3.2 mm in diameter (22 µl rotors) and with TOSS (total suppression of spinning sidebands). Orthophosphoric acid (H_3PO_4) was used to calibrate the phosphorus chemical shift scale (0 ppm). The applied acquisition parameters were: a spectral width of 50 kHz, a 90° pulse of 2.5 µs, a spin-lock field for cross polarization (CP) of 100 kHz, a contact time for CP of 1700 µs, an acquisition time of 20 ms, a recycle decay of 20 s and between 500 and 3000 accumulations. High-power proton dipolar decoupling during the acquisition time was set to 100 kHz. The Hartmann-Hahn condition for CP was calibrated accurately on the samples themselves.

3. Results and discussion

3.1. Adsorption of water on the anatase (101) and (001) surfaces

In order to validate the model used, the molecular and dissociative adsorption of water on the anatase (101) and (001) surfaces was studied. In the case of molecular adsorption, the oxygen atom of water is coordinated to a titanium atom on the surface. In case of dissociative adsorption, the hydroxyl group of the dissociated water molecule is attached to a titanium atom on the surface, while the remaining proton is bound to a twofold-coordinated oxygen atom nearby on the surface. The adsorption energy E_{ads} for the adsorbate on the clean surface is calculated as

$$E_{ads} = E_{adsorbate/surface} - (E_{adsorbate} + E_{surface})$$

where $E_{adsorbate/surface}$ is the energy of the adsorption complex, while $E_{adsorbate}$ and $E_{surface}$ are the energies of the isolated molecule and the clean surface, respectively. On the (101) surface, molecular adsorption (–83.5 kJ/mol) is clearly more stable than dissociative adsorption (–49.9 kJ/mol), which is in agreement with recently published results of –77.2 kJ/mol and –40.5 kJ/mol for molecular and dissociative adsorption, respectively [41]. The stability of the adsorption complexes is reversed on the (001) surface: dissociative adsorption (–186.5 kJ/mol) is more stable than molecular adsorption (–46.3 kJ/mol). This is also confirmed by previous studies from which adsorption energies of –79.5 and –62.8 kJ/mol for the molecular adsorption and –138.0 and –134.1 kJ/mol for the dissociative adsorption were obtained [19,42].

3.2. Adsorption of phosphonic acid derivatives on the anatase (101) and (001) surfaces

During the adsorption process oxygen atoms of the phosphonic acid coordinate with the titanium atoms on the TiO_2 surface. In this way, mono-, bi-, or tridentate structures are formed, depending on the number of oxygen atoms coordinated to the titanium atoms. Phosphonic acids (RPO_3H_2) adsorb as complete molecules on the TiO_2 surface (molecular or non-dissociative adsorption) or dissociate by relinquishing one (RPO_3H^-) or two protons (RPO_3^{2-}) to the surface (dissociative adsorption). Monodentate adsorption is possible in both a molecular and a dissociative fashion. Bidentate adsorption is only possible when one or both hydrogen atoms are dissociated to the surface and tridentate adsorption is only possible when both protons are dissociated to the surface. A systematic study of the different possible binding modes on the anatase (101) and (001) surfaces was performed using methylphosphonic acid (MPA), taking advantage of the computationally efficient methyl group; the results of this were then used as starting structures for adsorption complexes based on the larger butyl- (BPA) and phenylphosphonic acids (PPA).

As can be seen in Figure 1a, the corrugated anatase (101) surface is characterized by alternating rows of Ti atoms and rows of O atoms, the latter pointing out of the surface. Therefore, a tridentate binding mode is geometrically not possible on this surface. The most stable binding modes are presented in Figure 2 for MPA: a monodentate binding mode with two hydrogen bonds (101-M) and a bidentate binding mode with one hydrogen bond and one dissociated hydrogen atom (101-B), of which the latter is numerically slightly more stable than the former. Analogous results were obtained for BPA and PPA: the calculated adsorption energies are given in Table 2 and are compared with literature data. It is clear that the nature of the organic functional group does not influence the adsorption energy and that the difference in adsorption energy between both binding modes is small (limited to less than 10% of the energy value), suggesting that both binding modes can coexist on the surface. Nilsing *et al.* performed calculations on unsubstituted phosphonic acid (PA) and concluded that

monodentate binding mode is slightly more stable than bidentate [18], but again the numerical difference is quite small. Luschtinetz *et al.*, also working with PA, obtained a significantly larger difference in adsorption energies and reported an additional bidentate binding mode with both hydrogen atoms dissociated (101-B2) [16]; attempts to obtain this extra binding mode failed, as any starting structure favouring it spontaneously optimized to the bidentate binding mode with one hydrogen bond and one dissociated hydrogen atom, a structure which was also recently reported by Di Valentin *et al.* [43]. Our results are clearly also in good agreement with the recently published results of O'Rourke *et al.* [17]. The adsorption energy increases significantly when dispersion forces are taken into account in the energy calculations but the conclusions remain the same: the functional group does not influence the adsorption energy and both binding modes have a similar adsorption energy (with differences limited to less than 10% of the total energy), in agreement with Di Valentin *et al.* [43].

On the reactive (001) surface which is significantly flatter (Figure 1b) mono-, bi- and tridentate binding modes are in principle all possible. However, optimization of a number of monodentate binding modes always resulted in relaxation towards bidentate ones. The two most stable binding modes are a fully dissociated bidentate binding mode (001-B) and a tridentate binding mode (001-T), and both are shown in Figure 3; the associated adsorption energies are compiled in Table 3 and are compared with literature data. The bidentate binding mode is again numerically slightly more stable than the tridentate binding mode, even though the difference is well below 10% of the energy value. Overall, though, adsorption on the (001) surface is significantly more stable than on the (101) surface, for any of the functional groups; this is also reflected in O'Rourke's work on PA [17]. Including dispersion forces in the energy calculations significantly increases the adsorption energy but the conclusions again remain the same.

Calculated bond lengths of gas-phase methylphosphonic acid and of MPA in the various binding modes can be found in Table 4. These calculations were performed without taking dispersion forces into account in the energy calculations since including them was proven to have a negligible influence on the adsorption geometry of strongly adsorbed phosphonic acid molecules [43]; this was also recently reported for small organic molecules adsorbed on the rutile (110) surface [44]. As a consequence of adsorption on the anatase surface, the P–O bond lengths in (101-B) and (001-T) become almost equal. The O–Ti distances range from 1.90 Å to 2.07 Å and show a somewhat larger variation. The O–Ti bonds of (001-T) are elongated in order to accommodate the bonding with three of the Ti atoms of the surface.

3.2.1. Comparison of experimental and calculated ^{31}P chemical shifts

^{31}P NMR spectroscopy has been frequently applied to identify the binding mode(s) of covalently grafted phosphonic acid derivatives on TiO₂ surfaces [13,45,46]. However, since the shift of the ^{31}P peaks is not only affected by the binding mode, an unambiguous assignment has proven to be quite difficult: Brodard-Severac *et al.* found that each condensation between a P–OH group and a Ti–OH group leads to an upfield shift, but that interactions of the P=O groups with surface Lewis or Brønsted acidic sites leads to a downfield shift [15]. The calculated ^{31}P chemical shifts of the PAs in the different binding modes are presented in Table 5. The same conclusions can be drawn for all the PAs on the (101) surface: the monodentate binding mode is shifted upfield with respect to the bidentate binding mode. On the (001) surface, the tridentate binding mode is shifted upfield with respect to the bidentate binding mode.

Experimental ^{31}P chemical shifts of methylphosphonic acid (MPA), ethylphosphonic acid (EPA), butylphosphonic acid (BPA), octylphoshponic acid (OPA), dodecylphosphonic acid (DPA), octadecylphosphonic acid (ODPA) and phenylphoshponic acid (PPA) grafted onto TiO₂ can be found in Table 6 [the full spectra of the five compounds that were (re)measured for this work can be found in the Supplementary Information, Figures S1-S5]. All alkyl-substituted PAs grafted onto TiO₂ have a resonance at about 28 ppm, and MPA, EPA and DPA have an additional small resonance shifted downfield. For PPA, Mutin *et al.*, Guerrero *et al.* and our own work all agree on a resonance at about 13 ppm and a small additional resonance at about 20 ppm.

The references given in Table 6 all use P25 Degussa TiO₂ particles to prepare the modified surfaces. XRD analysis showed [47] that the ratio anatase/rutile in P25 Degussa TiO₂ is approximately 80/20 and the contribution of (101) facets on anatase is greater than 90% [48]. Therefore, the experimental ^{31}P chemical shifts should be compared with the shifts calculated for the (101) adsorption complexes (Table 5, columns 2 and 3). Comparison of the values calculated for grafted BPA (Table 5) with the experimental ones for grafted MPA, EPA, BPA, OPA, DPA and ODPA (Table 6) indicates that the upfield shift should be identified as a monodentate binding mode, while the additional resonance experimentally observed for MPA, EPA and DPA can be assigned to bidentate binding; a similar conclusion can be drawn for PPA. It may be clear that the simultaneous presence of the two binding modes on the anatase (101) surface, as inferred from these spectra, is completely in line with the small differences in adsorption energy obtained from the energy calculations (Table 3).

3.2.2. Comparison of experimental and calculated [17]O chemical shifts

Recent high-field ^{17}O NMR studies were able to differentiate between the P=O, P–O–H and P–O–Ti oxygen sites of PA monolayers on a TiO₂ anatase support [15]: Brodard-Severac *et al.* concluded that a mixture of several binding modes is present on the TiO₂ surface but no correlation was found

between the ^{31}P and ^{17}O NMR shifts. The calculated and experimental [17]O chemical shifts of isolated DPA and PPA are listed in Table 7. Although the shifts of the P=O oxygen atoms are insensitive to the nature of the hydrocarbon group, the [17]O shifts of the P–O–H oxygens do vary: the trends seen in the experimental values are clearly reproduced well. Due to the particular sensitivity of ^{17}O NMR parameters to hydrogen bonding, inclusion of the solvent may be an important factor when these calculated values are to be compared with experimental data. A comparison of the calculated and experimental [17]O chemical shifts of PPA adsorbed on TiO$_2$ is presented in Table 8: the lack of correlation between the experimental and calculated shifts suggests that solvent effects and higher surface coverages may be necessary in the computational model for a proper description of these parameters.

3.2.3. Comparison of experimental and calculated vibrational frequencies

Infrared spectroscopy is a popular technique to analyze the covalent attachment of monolayers on the surface of oxides. Several experimental studies were performed in order to characterize the binding mode of PAs on TiO$_2$ using IR spectra. Randon *et al.* [49] based his conclusion of tridentate binding on the fact that the three oxygen atoms cannot be differentiated in the IR spectrum. Guerrero *et al.* [46] also concluded that the main binding mode to the surface is tridentate, but they based this conclusion rather on the disappearance of the P=O stretching band near 1200-1250 cm^{-1}. Recently, Raman *et al.* [50] analysed the binding mode of phosphonic acid on different surfaces in function of the IR spectra: according to these authors, the observance of P–O and P=O stretches combined with the disappearance of the P–O–H stretch indicates bidentate binding, while the presence of P=O, P–O and shifted P–O–H stretches indicates monodentate binding. It is clear that the absence of a proper reference set of vibrational frequencies leads to ambiguous explanations and assignments.

Since the calculated vibrational frequencies of BPA in its different binding modes are very similar to those of MPA in its corresponding binding modes, only the results for MPA and PPA will be discussed. Calculated vibrational frequencies of isolated MPA and PPA and in the different binding modes are listed in Tables 9 and 10. Since the only major difference between MPA and PPA seems to be in the value for the P–C stretching mode, the following conclusions are valid for both MPA and PPA in the various binding modes.

The typical P=O stretch around 1260 cm^{-1} is only observed for the isolated molecules: irrespective of the binding mode, adsorption on the TiO$_2$ surface leads to a considerable shift of the P=O stretch to a lower wave number, and, consequently, the disappearance of this band cannot be used to assign a particular binding mode. On the anatase (101) surface, monodentate adsorption occurs with the doubly-bound phosphoryl oxygen leading to a considerable shift due to binding with the metal. The bidentate binding mode has similar P–O bond lengths (Table 4) and this is reflected in the calculated

vibrational frequencies: consequently, characterization of the binding mode on the (101) surface based on IR spectroscopy is not feasible. Gao *et al.* [13] obtained similar experimental results when studying the adsorption of ODPA on ZrO_2. Their conclusion was also that the disappearance of the P=O stretch cannot be interpreted as evidence for tridentate binding, because the different P–O stretching peaks greatly overlap and their precise location depends on the degree of hydrogen and metal bonding.

On the anatase (001) surface, the P=O bond in the bidentate binding mode is shifted towards about 1100 cm^{-1}, and symmetric and asymmetric P–O–Ti stretches can observed. Tridentate binding on (001) leads to vibrational frequencies for all P–O stretches in a narrow region of about 60 cm^{-1} since now all oxygen atoms are bonded to titanium atoms at the surface. Consequently, the characteristic vibrational frequency at about 1100 cm^{-1} associated with bidentate binding could be used to assign this binding mode on the (001) surface.

4. Conclusions

The adsorption of phosphonic acid derivatives (PAs) on TiO_2 anatase (101) and (001) surfaces was studied using the DFT/PBC formalism. In the model with low surface coverage used in this study, the functional groups (methyl, butyl, phenyl) do not influence the geometry and adsorption energy of the different binding modes. For the (101) surface, two stable binding modes were identified: a molecular monodentate binding mode and a monodissociated bidentate binding mode, which is numerically slightly more stable even though the difference between the two is small. A tridentate binding mode is not possible due to the particular geometry of the (101) surface. On the (001) surface, the two most stable binding modes are bidentate and tridentate, the latter in which both protons of the acid have been relinquished to the metal oxide surface. The binding modes on the (001) surface are considerably more stable than those on the (101) surface. Taking dispersion forces in the energy calculations into account increases the stability of all the binding modes but the geometries and relative stabilities of the binding modes remain unaltered.

[31]P and [17]O chemical shifts and vibrational frequencies were calculated for the different binding modes in order to correlate the obtained results with experimental data. Comparison of the calculated and experimental ^{31}P chemical shifts suggests that mono- and bidentate binding modes coexist on the anatase (101) surface. Since [17]O chemical shifts are far more sensitive to hydrogen bonding, future studies should focus on higher surface coverages and the inclusion of solvent effects in order to correlate calculated ^{17}O NMR parameters with experimental data.

Analysis of the vibrational frequencies associated with the different binding modes suggests that the disappearance of the P=O stretch can be used to indicate covalent bonding of the PAs to the TiO_2 surface, but that it cannot be used for a more detailed assignment of the precise binding mode. In

general, P–O stretching modes overlap too much to allow any unambiguous assignment of the binding mode based on IR spectra. One exception to this may be the characteristic vibrational frequency at about 1100 cm^{-1} associated with bidentate binding on anatase (001).

5. Acknowledgments

6. References

[1] V. Meynen, H.L. Castricum, A. Buekenhoudt, Curr. Org. Chem. 18 (2014) 2334.

[2] J. Amalric, P.H. Mutin, G. Guerrero, A. Ponche, A. Sotto, J.-P. Lavigne, J. Mater. Chem. 19 (2009) 141.

[3] N. Torres, S. Oh, M. Appleford, D.D. Dean, J.H. Jorgensen, J.L. Ong, C.M. Agrawal, G. Mani, Acta Biomater. 6 (2010) 3242.

[4] A. Hagfeldt, M. Grätzel, Chem. Rev. 95 (1995) 49.

[5] K. Kalyanasundaram, M. Grätzel, Coord. Chem. Rev. 77 (1998) 347.

[6] A. Hagfeldt, M. Grätzel, Acc. Chem. Res. 33 (2000) 269.

[7] S.P. Pujari, L. Scheres, A.T.M. Marcelis, H. Zuilhof, Angew. Chem. Int. Ed. 53 (2014) 6322.

[8] S. Marcinko, A.Y. Fadeev, Langmuir 20 (2004) 2270.

[9] L.A. Martini, G.F. Moore, R.L. Milot, L.Z. Cai, S.W. Sheehan, C.A. Schmuttenmaer, G.W. Brudvig, R.H. Crabtree, J. Phys. Chem. C 117 (2013) 14526.

[10] G. Guerrero, J.G. Alauzun, M. Granier, D. Laurencin, P.H. Mutin, Dalt. T. 42 (2013) 12569.

[11] R. Boissezon, J. Muller, V. Beaugeard, S. Monge, J.-J. Robin, RSC Adv. 4 (2014) 35690.

[12] C. Queffélec, M. Petit, P. Janvier, D.A. Knight, B. Bujoli, Chem. Rev. 112 (2012) 3777.

[13] W. Gao, L. Dickinson, C. Grozinger, F.G. Morin, L. Reven, Langmuir 12 (1996) 6429.

[14] P.H. Mutin, G. Guerrero, A. Vioux, J. Mater. Chem. 15 (2005) 3761.

[15] F. Brodard-Severac, G. Guerrero, J. Maquet, P. Florian, C. Gervais, P.H. Mutin, Chem. Mater. 20 (2008) 5191.

[16] R. Luschtinetz, J. Frenzel, T. Milek, G. Seifert, J. Phys. Chem. C 113 (2009) 5730.

[17] C. O'Rourke, D.R. Bowler, J. Phys. Condens. Matter 26 (2014) 195302.

[18] M. Nilsing, S. Lunell, P. Persson, L. Ojamäe, Surf. Sci. 582 (2005) 49.

[19] A. Vittadini, A. Selloni, F.P. Rotzinger, M. Grätzel, Phys. Rev. Lett. 81 (1998) 2954.

[20] X.G. Han, Q. Kuang, M.S. Jin, Z.X. Xie, L.S. Zheng, J. Am. Chem. Soc. 131 (2009) 3152.

[21] D.Q. Zhang, G.S. Li, J.C. Yu, Chem. Commun. (2009) 4381.

[22] P. Giannozzi, S. Baroni, N. Bonini, M. Calandra, R. Car, C. Cavazzoni, D. Ceresoli, G.L. Chiartti, M. Cococcioni, I. Dabo, A. Dal Corso, S. de Gironcoli, S. Fabris, G. Fratesi, R. Gebauer, U. Gerstmann, C. Gougoussis, A. Kokalj, M. Lazzeri, L. Martin-Samos, N. Marzari, F. Mauri, R. Mazzarello, S. Paolini, A. Pasquarello, L. Paulatto, C. Sbraccia, S. Scandolo, G. Sclauzero, A.P. Seitsonen, A. Smogunov, P. Umari, R.M. Wentzcovitch, J. Phys. Condens. Matter 21 (2009) 395502.

[23] Z. Wu, R.E. Cohen, Phys. Rev. B 73 (2006) 235116.

[24] P.E. Blöchl, Phys. Rev. B 50 (1994) 17953.

[25] N. Troullier, J.L. Martins, Phys. Rev. B 43 (1991) 1993.

[26] J.K. Burdett, T. Hughbanks, G.J. Miller, J.W. Richardson, J. V. Smith, J. Am. Chem. Soc. 109 (1987) 3639.

[27] F. Labat, P. Baranek, C. Domain, C. Minot, C. Adamo, J. Chem. Phys. 126 (2007) 154703.

[28] A. Beltran, J.R. Sambrano, M. Calatayud, F.R. Sensato, J. Andrés, Surf. Sci. 490 (2001) 116.

[29] T. Björkman, Comput. Phys. Commun. 182 (2011) 1183.

[30] A. Hussain, J. Gracia, B.E. Nieuwenhuys, J.W.H. Niemantsverdriet, ChemPhysChem 11 (2010) 2375.

[31] G. Shukri, H. Kasai, Surf. Sci. 619 (2014) 59.

[32] F. Labat, P. Baranek, C. Adamo, J. Chem. Theory Comput. 4 (2008) 341.

[33] M. Lazzeri, A. Vittadini, A. Selloni, Phys. Rev. B 63 (2001) 155409.

[34] Q. Chen, M. Liu, K. He, B. Li, Int. J. Photoenergy (2014) 816234.

[35] V.M. Bermudez, J. Phys. Chem. C 115 (2011) 6741.

[36] C.J. Pickard, F. Mauri, Phys. Rev. B 63 (2001) 245101.

[37] D. Müller, E. Jahn, G. Ladweg, U. Haubenreisser, Chem. Phys. Lett. 109 (1984) 332.

[38] C. Gervais, M. Profeta, V. Lafond, C. Bonhomme, T. Azaïs, H. Mutin, C.J. Pickard, F. Mauri, F. Babonneau, Magn. Reson. Chem. 42 (2004) 445.

[39] S. Grimme, J. Comput. Chem. 27 (2006) 1787.

[40] V. Barone, M. Casarin, D. Forrer, M. Pavone, M. Sambi, A. Vittadini, J. Comput. Chem. 30 (2009) 934.

[41] C.E. Patrick, F. Giustino, Phys. Rev. Appl. 2 (2014) 014001.

[42] R. Erdogan, O. Ozbek, I. Onal, Surf. Sci. 604 (2010) 1029.

[43] C. Di Valentin, D. Costa, J. Phys. Chem. C 116 (2012) 2819.

[44] M.J. Tillotson, P.M. Brett, R.A. Bennett, R. Grau-Crespo, Surf. Sci. 632 (2015) 142.

[45] P.H. Mutin, V. Lafond, A.F. Popa, M. Granier, L. Markey, A. Dereux, Chem. Mater. 16 (2004) 5670.

[46] G. Guerrero, P.H. Mutin, A. Vioux, Chem. Mater. 13 (2001) 4367.

[47] H. Jensen, K.D. Joensen, J.-E. Jorgensen, J.S. Pedersen, E.G. Sogaard, J. Nanopart. Res. 6 (2004) 519.

[48] M. V. Dozzi, E. Selli, Catalysts 3 (2013) 455.

[49] J. Randon, P. Blanc, R. Paterson, J. Membr. Sci. 98 (1995) 119.

[50] A. Raman, R. Quinones, L. Barriger, R. Eastman, A. Parsi, E.S. Gawalt, Langmuir 26 (2010) 1747.

Table 1. Selected geometrical parameters (bond lengths in Å and angles in degrees) of the relaxed top layers of the anatase (101) and (001) surfaces. Atom labels refer to Figure 1.

Anatase (101)	This work	Ref. 32[a]	Ref. 33[b]
Ti1-O1	1.855	1.845	1.866
Ti2-O1	1.818	1.830	1.823
Ti2-O2	1.779	1.779	1.786
Ti2-O3	1.972	1.981	1.975
Ti2-O4	2.038	2.068	2.078
Anatase (001)	**This work**	**Ref. 32[a]**	**Ref. 34[c]**
Ti1-O1	2.210	2.202	2.207
O1-Ti2	1.755	1.758	1.738
Ti1-O1-Ti2	145.4	146.0	146.7

[a]DFT/PBE, plane waves, pseudopotential, six O-Ti-O layers.
[b]DFT/GGA, plane waves, pseudopotential, three O-Ti-O layers.
[c]DFT/B3LYP, Gaussian basis set, pseudopotential, four O-Ti-O layers.

Table 2. Calculated adsorption energies (E_{ads} in kJ/mol) of phosphonic acid derivatives on the anatase (101) surface.

	Adsorbate	101-M	101-B	101-B2
This work	MPA	-184.19	-190.71	
This work	BPA	-184.79	-190.98	
This work	PPA	-176.65	-187.28	
Nilsing *et al.*[a]	PA	-197.07	-186.19	
Luschtinetz *et al.*[b]	PA	-189.37	-260.52	-276.83
O'Rourke *et al.*[c]	PA	-163.06	-175.60	
Di Valentin *et al.*[d]	BPA	-219.99	-241.21	
This work[e]	MPA	-226.90	-245.52	
This work[e]	BPA	-229.39	-248.58	
This work[e]	PPA	-228.19	-252.37	

[a]DFT/B3LYP, Gaussian-type basis set. [b]DFTB/PBE, localized atom-centered basis set. [c]DFT/PW91, plane waves basis set. [d]DFT/B3LYP-D, Gaussian-type basis set. [e]Including dispersion contribution.

Table 3. Calculated adsorption energies (E_{ads} in kJ/mol) of phosphonic acid derivatives on the anatase (001) surface.

	Adsorbate	001-B	001-T
This work	MPA	-280.37	-259.66
This work	BPA	-277.36	-259.05
This work	PPA	-285.29	-256.19
O'Rourke et al.[a]	PA	-309.72	-288.49
This work[b]	MPA	-345.75	-326.58
This work[b]	BPA	-339.36	-329.33
This work[b]	PPA	-345.97	-325.91

[a]DFT/PW91, plane waves basis set. [b]Including dispersion contribution.

Table 4. Calculated bond distances (in Å) of free methylphosphonic acid (MPA) and of adsorption complexes on the anatase (101) and (001) surfaces with different binding modes.

	MPA	(101) surface		(001) surface	
	MPA	101-M	101-B	001-B	001-T
P-O1	1.613	1.558	1.562	1.510	1.556
P-O2	1.613	1.560	1.553	1.576	1.558
P-O3	1.480	1.533	1.542	1.586	1.566
O1-Ti	-	-	-	-	2.001
O2-Ti	-	-	1.969	1.908	2.067
O3-Ti	-	1.943	1.969	1.900	1.908

Table 5. Calculated ^{31}P chemical shifts (in ppm) of adsorption complexes on the anatase (101) and (001) surfaces with different binding modes.

	101-M	101-B	001-B	001-T
MPA	26.5	29.7	27.0	24.6
BPA	26.6	31.7	28.8	25.4
PPA	11.8	18.0	15.9	12.5

Table 6. Experimental ^{31}P chemical shifts of phosphonic acid derivatives grafted on TiO_2; the value between brackets indicates the presence of a small, additional resonance.

	Gao *et al.* [13]	Mutin *et al.* [45]	Guerrero *et al.* [46]	This work
MPA				29 (37)
EPA				28 (38)
BPA				28
OPA				28
DPA		28.3 (33.4)		
ODPA	28.0			
PPA		13.6 (19.4)	13 (19)	13 (21)

Table 7. Calculated and experimental [17]O chemical shifts (in ppm) of isolated DPA and PPA.

		This work	Exp. [15]
DPA	O=P	105	103
	P-O-H	63	80
PPA	O=P	108	103
	P-O-H	70	91
	P-O-H	58	74

Table 8. Calculated and experimental [17]O chemical shifts (in ppm) of PPA adsorbed on TiO_2. Atom labels refer to Figures 2 and 3.

|	This work		Exp. [15]	
101 surface, monodentate	P-O-Ti (O3)	241	P=O	103
	P-O-H (O1)	88	P-O-Ti	185
	P-O-H (O2)	87	P-O-H	80
101 surface, bidentate	P-O-Ti (O2)	262	P-O-Ti	190
	P-O-Ti (O3)	223	P-O-Ti	170
	P-O-H (O1)	99	P=O	113
			P-O-H	80
001 surface, bidentate	O=P (O1)	144		
	P-O-Ti (O2)	313		
	P-O-Ti (O3)	316		
001 surface, tridentate	P-O-Ti (O3)	302		
	P-O-Ti (O2)	232		
	P-O-Ti (O1)	300		

Table 9. Calculated vibrational frequencies (in cm^{-1}) of isolated MPA and its adsorption complexes on the anatase (101) and (001) surfaces in the different binding modes.

Mode	MPA	101-M	101-B	001-B	001-T
ν(P-C)	721	765	770	769	764
ν(P=O)	1253			1109	
ν(P-O)$_{POTi}$		1072			
ν(P-O$_{asym}$)	910	1051			
ν(P-O$_{sym}$)	877	969			
ν(PO$_3$)			1037		993
			1005		963
			970		940
ν(P-O-Ti$_{sym}$)				941	
ν(P-O-Ti$_{asym}$)				913	

**Table 10.** Calculated vibrational frequencies (in cm^{-1}) of isolated PPA and its adsorption complexes on the anatase (101) and (001) surfaces in the different binding modes.

Mode	PPA	101-M	101-B	001-B	001-T
ν(P-C)	1123	1124	1117	1136	1100
ν(P=O)	1264			1101	
ν(P-O-Ti)		1061			
ν(P-O-H$_{asym}$)	870	1046			
ν(P-O-H$_{sym}$)	821	934			
ν(PO$_3$)			1033		971
			1001		955
			945		915
ν(P-O-Ti$_{sym}$)				928	
ν(P-O-Ti$_{asym}$)				902	

Figure 1. Numbering of the atoms in the top layers of (a) the anatase (101) and (b) the anatase (001) surfaces. Red and grey spheres represent oxygen and titanium atoms, respectively.
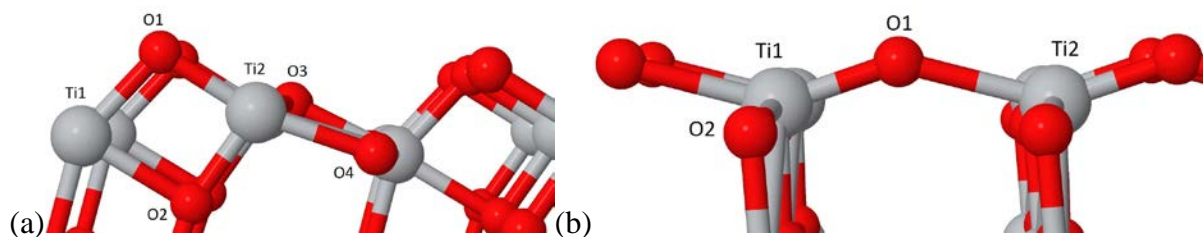
Figure 2. (a) Side and (b) top views of the most stable monodentate (101-M) binding modes on the anatase (101) surface; (c) side and (d) top views of the most stable bidentate (101-B) binding modes on the anatase (101) surface. White and orange spheres represent hydrogen and phosphorus atoms, respectively.
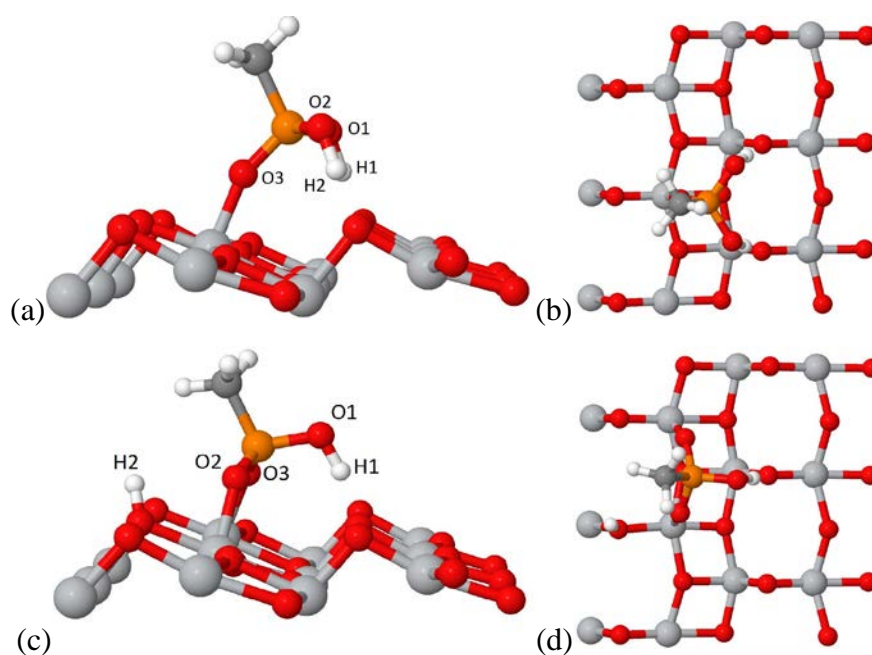
Figure 3. (a) Side and (b) top views of the most stable bidentate (001-B) binding modes on the anatase (001) surface; (c) side and (d) top views of the most stable tridentate (001-T) binding modes on the anatase (001) surface.